**Proceedings of the ASME 2012 International Design Engineering Technical Conferences &
Computers and Information in Engineering Conference
IDETC/CIE 2012
August 12-15, 2012, Chicago, IL, USA**

DETC2012-70485

DESIGN AND QUATERNION-BASED ATTITUDE CONTROL OF THE OMNICOPTER MAV USING FEEDBACK LINEARIZATION

Yangbo Long, Sean Lyttle, Nicholas Pagano, David J. Cappelleri*
Multi-Scale Robotics and Automation Laboratory
Department of Mechanical Engineering
Stevens Institute of Technology
Hoboken, NJ 07030
Email: {ylong1, slyttle, npagano, David.Cappelleri} @stevens.edu

ABSTRACT

In this paper, we present the design of the Omnicopter, a micro aerial vehicle (MAV) with two central counter-rotating coaxial propellers for thrust and yaw control and three perimeter-mounted variable angle ducted fans to control roll and pitch. First, a dynamic model of the robot is established using the Euler-Lagrange formalism. Next, we focus on the attitude control for a special operating case of the Omnicopter with fixed vertical positions of the surrounding ducted fans. A nonlinear model is represented in state space using the quaternion and angular velocity as state variables, which simplifies the system dynamics. Based on this model, a feedback linearization controller is developed, which renders the system linear and controllable from an input-output point of view. The zero dynamics problem is also analyzed. Finally, simulations are carried out and the results illustrate that the attitude stabilization task for the Omnicopter is achieved.

I. INTRODUCTION

The interest in autonomous micro aerial vehicles (MAV) has been steadily growing in the last few decades. These kinds of vehicles can be used in tasks such as search and rescue, surveillance, building exploration, manipulation, communication relaying, inspection and mapping. Their small size provide for low acoustic signatures and radar cross-sections that are ideal for stealth operations [1]. In the last few years, MAVs in the tri-coptor [2–4] and quadrotor [5–10] configurations have been highlighted in many papers. There has also been some recent work on unique MAV configurations that use gyroscopic moments for attitude control [1, 11, 12]. In the first part of this paper, we will present our novel VTOL (Vertical Take-Off and Landing) MAV design called the *Omnicopter* (Fig.1) along with its dynamic model based on the Euler-Lagrange formalism. The system model is represented in state space using quaternion and angular velocity in the body frame as state variables.

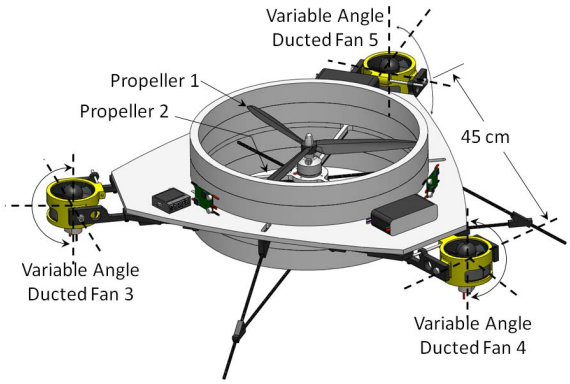

FIGURE 1. Omnicopter MAV Schematic

Different control techniques have been applied to the tri-copter and quadrotor MAV configurations, such as PID, LQR,

*Address all correspondence to this author.

H_∞ and sliding mode control [5, 7–9]. The quadrotor MAV is based on the VTOL concept and is viewed as an ideal platform to develop control laws, due to its simple structure, agility and controllability. In previous work, the quadrotor MAV has also been controlled using the feedback linearization technique. In [13], a dynamic feedback controller was developed to make the input-output problem solvable for a nonlinear dynamic model. In [14], a feedback linearization-based controller with a sliding mode observer was designed for the quadrotor MAV. An adaptive observer was added to the control system to estimate the effect of external disturbances. In the second part of this paper, we focus on the attitude control of the Omnicopter for a special operating case that is similar to that of the quadrotor, also using feedback linearization. Based on the Omnicopter nonlinear model, we design a quaternion-based attitude control algorithm. The zero dynamics problem is also analyzed. Finally, simulations are carried out and results presented to prove the feasibility of the proposed controller. The major conclusions of the paper are then drawn and directions for future work are presented.

II. OMNICOPTER DESIGN

A schematic of the Omnicopter configuration MAV is shown in Fig. 1. Drawing inspiration from omnidirectional wheels, the Omnicopter design allows for agile movements in any planar direction with fixed (zero) yaw, pitch and roll angles. It has five propellers: two fixed major coaxial counter-rotating propellers in the center used to provide most of the thrust and adjust the yaw angle, and three adjustable angle small ducted fans located in three places surrounding the airframe to control its roll and pitch. Unlike quadrotor or typical trirotor MAVs [2, 3], the Omnicopter has different motion principles and control modes. Increasing or decreasing the five propeller's speeds together generates vertical motion. The yaw movement results from different speeds of the two counter-rotating coaxial propellers. The roll and pitch motions can be generated using two methods (M1 and M2), as shown in Fig. 2. For M1, fixed ducted fan angles with varying fan speeds are used; and for M2, varying both the angles and speeds of the ducted fans are employed for attitude control. With method M1, the difference between the speeds of Fan 4 and 5 produces roll motion coupled with lateral motion. The pitch rotation and the corresponding lateral motion result from the difference between Fan 3's speed and the collective effect of rotation of Fan 4 and 5. The second control method (M2) is to adjust the angles of the surrounding ducted fans, with the fan's speeds variable or fixed, to generate the roll and pitch motions. This control method, or operating mode, allows for lateral force vectors to be applied to the airframe while keeping a planar, zero attitude configuration. This design feature is unique to the Omnicopter, when compared to traditional quadrotor and tri-copter designs (Fig. 3). This is advantageous in outdoor operating scenarios when steady point-to-point lateral translation in the presence of external disturbances, such as wind, is needed, for example in accurate remote sensing applications.

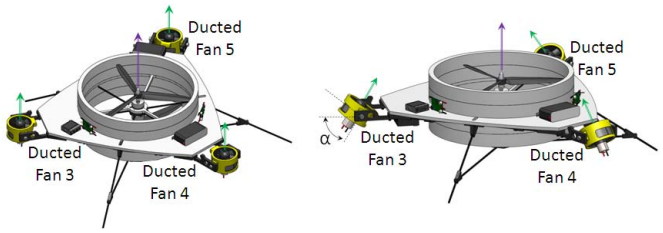

FIGURE 2. Omnicopter Control Methods. M1: Fixed ducted fan angles with varying speeds (left); M2: Variable ducted fan angles and variable speeds (right)

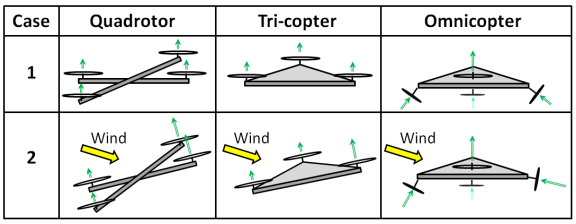

FIGURE 3. Comparison of between the Quadrotor, Tricopter, and Omnicopter MAVs. Case 1: Hover; Case 2: Lateral Translation in the presence of disturbances (wind). The Omnicopter can maintain zero roll and pitch attitude for Case 2 while the other configurations cannot.

III. SYSTEM MODELING

The coordinate systems and free body diagram for the Omnicopter are shown in Fig. 4. The inertial frame $I = \{I_x, I_y, I_z\}$ is considered fixed with respect to the earth, with axis I_z pointing downward. Let $B = \{B_x, B_y, B_z\}$, which is attached to the center of mass of the Omnicopter MAV, be the body frame, where the B_x axis is in the forward flight direction, B_y is perpendicular to B_x and positive to the right in the body plane, whereas B_z is orthogonal to the plane formed by B_x and B_y and points vertically downwards during perfect hover. We use Z-Y-X Euler angles to model the rotation of the Omnicopter MAV in the inertial frame. The airframe orientation is given by a rotation matrix $\boldsymbol{R}$: $B \to I$, where $\boldsymbol{R} \in \mathrm{SO}(3)$ is an orthonormal rotation matrix. To get from B to I, we first rotate about B_z by the yaw angle, ψ, then rotate about the intermediate Y-axis by the pitch angle, θ, and finally rotate about the I_x axis by the roll angle, ϕ. This rotation matrix is given by [15]:

$$\boldsymbol{R} = \begin{bmatrix} c\psi c\theta & c\psi s\theta s\phi - s\psi c\phi & c\psi s\theta c\phi + s\psi s\phi \\ s\psi c\theta & s\psi s\theta s\phi + c\psi c\phi & s\psi s\theta c\phi - s\phi c\psi \\ -s\theta & c\theta s\phi & c\theta c\phi \end{bmatrix}$$

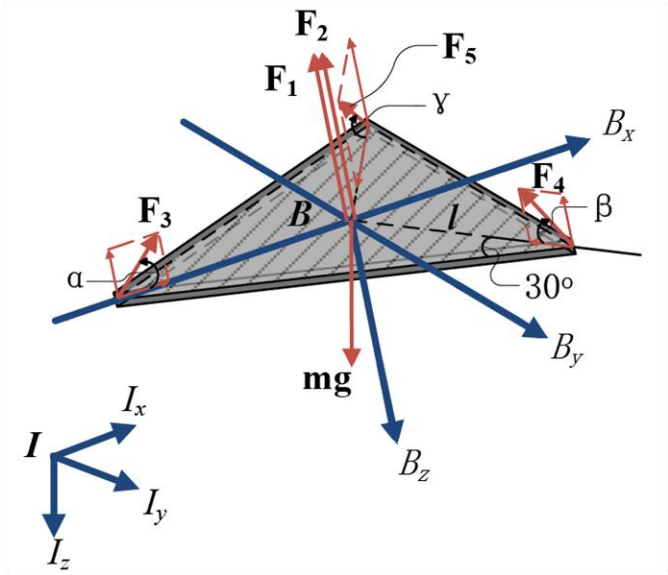

FIGURE 4. Omnicopter MAV free body diagram (*B*: Body-fixed coordinate frame; *I*: Inertial reference frame)

where $c = \cos$ and $s = \sin$.

The derivatives with respect to time of the roll, pitch and yaw angles can be expressed in the form

$$\begin{bmatrix} \dot{\phi} \\ \dot{\theta} \\ \dot{\psi} \end{bmatrix} = \begin{bmatrix} 1 & \sin\phi\tan\theta & \cos\phi\tan\theta \\ 0 & \cos\phi & -\sin\phi \\ 0 & \sin\phi\sec\theta & \cos\phi\sec\theta \end{bmatrix} \begin{bmatrix} \omega_x \\ \omega_y \\ \omega_z \end{bmatrix} \tag{1}$$

where $\boldsymbol{\omega} = [\omega_x\ \omega_y\ \omega_z]^T$ is the angular velocity in the body frame.

A. Modeling with Euler-Lagrange Formalism

We choose the generalized coordinates vector to be $\boldsymbol{q} = [\boldsymbol{\varepsilon}; \boldsymbol{\zeta}] = [\varepsilon_1\ \varepsilon_2\ \varepsilon_3\ \phi\ \theta\ \psi]^T$, where $\boldsymbol{\varepsilon} = [\varepsilon_1\ \varepsilon_2\ \varepsilon_3]^T$ represents the position of the Omnicopter mass center expressed in the inertial frame *I*, and $\boldsymbol{\zeta} = [\phi\ \theta\ \psi]^T$ is the Euler angles vector. The generalized force vector about the generalized coordinates is $\boldsymbol{\Gamma} = [\boldsymbol{F}; \boldsymbol{\tau}] = [F_{\varepsilon_1}\ F_{\varepsilon_2}\ F_{\varepsilon_3}\ \tau_\phi\ \tau_\theta\ \tau_\psi]^T$. The generalized forces of the translational movement can be obtained as the following:

$$\boldsymbol{F} = \boldsymbol{R} \begin{bmatrix} k_{F_2}(\Omega_3^2 c\alpha - (\Omega_4^2 c\beta + \Omega_5^2 c\gamma)s30^\circ) \\ k_{F_2}(\Omega_5^2 c\gamma - \Omega_4^2 c\beta)c30^\circ \\ -k_{F_1}(\Omega_1^2 + \Omega_2^2) - k_{F_2}(\Omega_3^2 s\alpha + \Omega_4^2 s\beta + \Omega_5^2 s\gamma) \end{bmatrix} \tag{2}$$

where k_{F1} and k_{F2} are factors that relate the central propeller's speeds to thrusts, the 30° angle is shown in Fig. 4, and Ω_i denotes each propeller's speed, i = 1, 2, ⋯, 5.

The nonconservative torques acting on the Omnicopter MAV result firstly from the thrust imbalance of the three surrounding ducted fans by:

$$\begin{aligned} \tau_{x_1} &= (F_5 \sin\gamma - F_4 \sin\beta) l \cos 30^\circ \\ \tau_{y_1} &= (F_4 \sin\beta + F_5 \sin\gamma) l \sin 30^\circ - F_3 (\sin\alpha) l \\ \tau_{z_1} &= 0 \end{aligned}$$

Secondly, torques result from the gyroscopic effects due to the propellers rotation by assuming that the upper propeller in the center rotates CCW (counterclockwise) and the lower one rotates CW (clockwise):

$$\begin{aligned} \tau_{x_2} &= J_p \omega_y (\Omega_1 - \Omega_2) \\ \tau_{y_2} &= J_p \omega_x (\Omega_2 - \Omega_1) \\ \tau_{z_2} &= 0 \end{aligned}$$

where J_p is the propeller inertia.

The final component of the torques are due to the reactive torque imbalance of propeller 1 and 2:

$$\begin{aligned} \tau_{x_3} &= 0 \\ \tau_{y_3} &= 0 \\ \tau_{z_3} &= k_M (\Omega_1^2 - \Omega_2^2) \end{aligned}$$

where k_M is a factor that relates the central propeller's speeds to the counter torque.

Thus, the total torques acting about the x, y and z axes are

$$\begin{aligned} \tau_x &= (F_5 s\gamma - F_4 s\beta) l c30^\circ + J_p \omega_y (\Omega_1 - \Omega_2) \\ \tau_y &= (F_4 s\beta + F_5 s\gamma) l s30^\circ - F_3 s\alpha l + J_p \omega_x (\Omega_2 - \Omega_1) \\ \tau_z &= k_M (\Omega_1^2 - \Omega_2^2) \end{aligned} \tag{3}$$

From Eq. (1), we can obtain

$$\boldsymbol{\omega} = \begin{bmatrix} 1 & 0 & -\sin\theta \\ 0 & \cos\phi & \sin\phi\cos\theta \\ 0 & -\sin\phi & \cos\phi\cos\theta \end{bmatrix} \begin{bmatrix} \dot{\phi} \\ \dot{\theta} \\ \dot{\psi} \end{bmatrix} \tag{4}$$

Since the Omnicopter MAV is symmetric with respect to the B_xB_y and B_xB_z planes, we can assume that the inertia matrix is diagonal

$$\boldsymbol{J} = \begin{bmatrix} I_{xx} & 0 & 0 \\ 0 & I_{yy} & 0 \\ 0 & 0 & I_{zz} \end{bmatrix} \tag{5}$$

According to Eq. (4) and Eq. (5), we can obtain the angular momentum relative to the mass center o

$$\boldsymbol{H}_o = \boldsymbol{J}\boldsymbol{\omega}$$

Then the kinetic energy equation can be expressed as follows:

$$T = \tfrac{1}{2} m \boldsymbol{v}_o \cdot \boldsymbol{v}_o + \tfrac{1}{2} \boldsymbol{\omega} \cdot \boldsymbol{H}_o$$

where $\boldsymbol{v}_o$ is the velocity of the Omnicopter in the inertial frame. The potential energy is:

$$V = -mg\varepsilon_3$$

Based on the kinetic and potential energy equations, we can derive the equations of motion using the Euler-Lagrange formalism [16]

$$\Gamma_j = \tfrac{d}{dt}\left(\tfrac{\partial T}{\partial \dot{q}_j}\right) - \tfrac{\partial T}{\partial q_j} + \tfrac{\partial V}{\partial q_j}$$

where q_j denotes a component of the generalized coordinates vector, j = 1, 2, $\cdots$, 6.

Finally, the equations of motion are obtained as the following:

$$\begin{aligned} &m\ddot{\varepsilon}_1 = F_{\varepsilon_1} \\ &m\ddot{\varepsilon}_2 = F_{\varepsilon_2} \\ &m\ddot{\varepsilon}_3 - mg = F_{\varepsilon_3} \\ &I_{xx}\dot{\omega}_x - (I_{yy} - I_{zz})\omega_y\omega_z = \tau_x \\ &I_{yy}\dot{\omega}_y - (I_{zz} - I_{xx})\omega_x\omega_z = \tau_y \\ &I_{zz}\dot{\omega}_z - (I_{xx} - I_{yy})\omega_x\omega_y = \tau_z \end{aligned} \tag{6}$$

In Eq. (6), F_{ε_1}, F_{ε_2} and F_{ε_3} represent the generalized forces of the translational movement in Eq. (2) for a complete system model.

In this paper, we focus on an Omnicopter being controlled with method M1 (Fig.2(left)): fixed angle ducted fans with varying speeds. We assume that the surrounding ducted fans point vertically upwards, thus the angles α, β and γ in Eq. (2) become 90°. In this case, the B_x and B_y components of F become 0, and the equations of motion of the translational subsystem become

$$\begin{aligned} &m\ddot{\varepsilon}_1 = -(c\psi s\theta c\phi + s\psi s\phi)U_1 \\ &m\ddot{\varepsilon}_2 = -(s\psi s\theta c\phi - c\psi s\phi)U_1 \\ &m\ddot{\varepsilon}_3 - mg = -c\theta c\phi U_1 \end{aligned}$$

where $U_1 = k_{F_1}(\Omega_1^2 + \Omega_2^2) + k_{F_2}(\Omega_3^2 + \Omega_4^2 + \Omega_5^2)$.

Now similar in dynamics to the quadrotor MAV, as shown in [5], the linear equations of motion are simple in the inertial reference frame, while the angular equations are advantageous to be expressed in the body-fixed coordinate frame. Therefore, the translational equations of motion of the Omnicopter MAV are expressed in the inertial frame, while the rotational equations are expressed in the body-fixed frame (τ_x, τ_y and τ_z in Eq. (6)).

B. Quaternion-based State Space Representation

For the attitude control of the Omnicopter MAV, the rotational movement can be extracted and simplified in order to design a feedback linearization controller. As stated above, the angles α, β and γ in Eq. (2) and (3) are 90°. The gyroscopic effects (τ_{x_2}, τ_{y_2} and τ_{z_2}) included in Eq. (3) then become zero in a simplified version of rotational dynamics. Then the simplified attitude dynamics are shown as follows:

$$\begin{aligned} \dot{\omega}_x &= a_1\omega_y\omega_z + b_1U_2 \\ \dot{\omega}_y &= a_2\omega_x\omega_z + b_2U_3 \\ \dot{\omega}_z &= a_3\omega_x\omega_y + b_3U_4 \end{aligned} \tag{7}$$

where

$$\begin{aligned} U_2 &= k_{F_2}(\Omega_5^2 - \Omega_4^2) \\ U_3 &= k_{F_2}[(\Omega_4^2 + \Omega_5^2)\sin 30° - \Omega_3^2] \\ U_4 &= k_M(\Omega_1^2 - \Omega_2^2) \end{aligned}$$

and $a_1 = \frac{I_{yy}-I_{zz}}{I_{xx}}$, $a_2 = \frac{I_{zz}-I_{xx}}{I_{yy}}$, $a_3 = \frac{I_{xx}-I_{yy}}{I_{zz}}$, $b_1 = \frac{l\cos 30°}{I_{xx}}$, $b_2 = \frac{l}{I_{yy}}$, $b_3 = \frac{1}{I_{zz}}$.

Although the Euler angles representation is more understandable and straightforward than the quaternion representation, it has a singularity problem when the pitch angle, θ, approaches 90° [17]. In addition, the attitude dynamics will be largely simplified when using the quaternion instead of Euler angles as the state variables. Due to these reasons, the quaternion-based dynamic modeling method has been widely used in spacecrafts' control [18]. Therefore, we adopt the quaternion instead of Euler angles to establish the state equations. Let $\boldsymbol{Q} = [q_0\ q_1\ q_2\ q_3]^T$ be the *attitude quaternion* of the Omnicopter MAV, then the relationship between the quaternion and the angular velocity can be expressed as follows [19]:

$$\begin{bmatrix} \dot{q}_0 \\ \dot{q}_1 \\ \dot{q}_2 \\ \dot{q}_3 \end{bmatrix} = \frac{1}{2} \begin{bmatrix} -q_1 & -q_2 & -q_3 \\ q_0 & -q_3 & q_2 \\ q_3 & q_0 & -q_1 \\ -q_2 & q_1 & q_0 \end{bmatrix} \begin{bmatrix} \omega_x \\ \omega_y \\ \omega_z \end{bmatrix} \tag{8}$$

Now we can define the state variable to be $\boldsymbol{x} = [q_0\ q_1\ q_2\ q_3\ \omega_x\ \omega_y\ \omega_z]^T$. Using Eq. (7) and (8), we get a system of nonlinear differential equations which is described in state space form by

$$\begin{aligned} \dot{\boldsymbol{x}} &= f(\boldsymbol{x}) + g(\boldsymbol{x})\boldsymbol{u} \\ \boldsymbol{y} &= h(\boldsymbol{x}) \end{aligned} \tag{9}$$

where

$$f(\boldsymbol{x}) = \begin{bmatrix} -\frac{1}{2}\omega_x q_1 - \frac{1}{2}\omega_y q_2 - \frac{1}{2}\omega_z q_3 \\ \frac{1}{2}\omega_x q_0 + \frac{1}{2}\omega_z q_2 - \frac{1}{2}\omega_y q_3 \\ \frac{1}{2}\omega_y q_0 - \frac{1}{2}\omega_z q_1 + \frac{1}{2}\omega_x q_3 \\ \frac{1}{2}\omega_z q_0 + \frac{1}{2}\omega_y q_1 - \frac{1}{2}\omega_x q_2 \\ a_1\omega_y\omega_z \\ a_2\omega_x\omega_z \\ a_3\omega_x\omega_y \end{bmatrix}$$

$$g(\boldsymbol{x}) = \begin{bmatrix} g_1(\boldsymbol{x}) & g_2(\boldsymbol{x}) & g_3(\boldsymbol{x}) \end{bmatrix} = \begin{bmatrix} \mathbf{0}_{4\times 3} \\ b_1 & 0 & 0 \\ 0 & b_2 & 0 \\ 0 & 0 & b_3 \end{bmatrix}$$

and $\boldsymbol{u} = [U_2\ U_3\ U_4]^T$ is the input of the attitude subsystem, $\boldsymbol{y} = [h_1(\boldsymbol{x})\ h_2(\boldsymbol{x})\ h_3(\boldsymbol{x})]^T = [q_1\ q_2\ q_3]^T$ is chosen to be the output of the system. Since the unit quaternion satisfies the constraint, $q_0^2 + q_1^2 + q_2^2 + q_3^2 = 1$, the state variable q_0 can be solved.

IV. FEEDBACK LINEARIZATION CONTROLLER

This section deals with the design of a quaternion-based feedback control scheme for the purpose of transforming the nonlinear system (9) into a linear and controllable system. Each of the output components is differentiated a sufficient number of times until a control input component appears in the resulting equation. Using the Lie derivative, input-output linearization can transform the nonlinear system into a linear system. Then we can apply a linear control law for the linearized system.

A. Feedback Linearization

Following the method in [13], the vector relative degree of the system (9), $[r_1\ r_2\ r_3]^T = [2\ 2\ 2]^T$, while the dimension of the system is 7. Since $r_1+r_2+r_3 = 6 < 7$, the nonlinear system can be input-output linearized only. Thus, we have

$$\begin{bmatrix} {y_1}^{(r_1)} \\ {y_2}^{(r_2)} \\ {y_3}^{(r_3)} \end{bmatrix} = \boldsymbol{D}(\boldsymbol{x}) + \boldsymbol{E}(\boldsymbol{x})\boldsymbol{u}$$

where $\boldsymbol{D}(\boldsymbol{x})$ and $\boldsymbol{E}(\boldsymbol{x})$ are computed as:

$$\boldsymbol{D}(\boldsymbol{x}) = \begin{bmatrix} L_f^{r_1} h_1(\boldsymbol{x}) \\ L_f^{r_2} h_2(\boldsymbol{x}) \\ L_f^{r_3} h_3(\boldsymbol{x}) \end{bmatrix}$$

$$\boldsymbol{E}(\boldsymbol{x}) = \begin{bmatrix} L_{g_1} L_f^{r_1-1} h_1(\boldsymbol{x}) & \cdots & L_{g_3} L_f^{r_1-1} h_1(\boldsymbol{x}) \\ \vdots & \ddots & \vdots \\ L_{g_1} L_f^{r_3-1} h_3(\boldsymbol{x}) & \cdots & L_{g_3} L_f^{r_3-1} h_3(\boldsymbol{x}) \end{bmatrix} \qquad (10)$$

where the Lie derivatives are defined as:

$$L_f h_i(\boldsymbol{x}) = \sum_{j=1}^{7} \frac{\partial h_i}{\partial x_i} f(\boldsymbol{x}),$$

$$L_f^{r_i} h_i(\boldsymbol{x}) = L_f(L_f^{r_i-1} h_i(\boldsymbol{x})) = \sum_{j=1}^{7} \frac{\partial L_f^{r_i-1} h_i}{\partial x_i} f(\boldsymbol{x}),$$

and $$L_{g_i} L_f^{r_i-1} h_i(\boldsymbol{x}) = \sum_{j=1}^{7} \frac{\partial L_f^{r_i-1} h_i}{\partial x_i} g_i(\boldsymbol{x}), i = 1,2,3.$$

The feedback linearization is feasible if and only if the matrix $\boldsymbol{E}(\boldsymbol{x})$ is nonsingular, which means that $\det(\boldsymbol{E}(\boldsymbol{x})) \neq 0$. We can obtain the matrix $\boldsymbol{E}(\boldsymbol{x})$ by calculating Eq. (10)

$$\boldsymbol{E}(\boldsymbol{x}) = \frac{1}{2}\begin{bmatrix} b_1 q_0 & -b_2 q_3 & b_3 q_2 \\ b_1 q_3 & b_2 q_0 & -b_3 q_1 \\ -b_1 q_2 & b_2 q_1 & b_3 q_0 \end{bmatrix} \qquad (11)$$

From (11), we know that

$$det(\boldsymbol{E}(\boldsymbol{x})) = \tfrac{1}{8} b_1 b_2 b_3 (q_0^2 + q_1^2 + q_2^2 + q_3^2) q_0 = \tfrac{1}{8} b_1 b_2 b_3 q_0$$

When $q_0 \neq 0$, the matrix $\boldsymbol{E}(\boldsymbol{x})$ is nonsingular and the input-output linearization problem is solvable for the nonlinear system (9). Letting $\boldsymbol{v} = \boldsymbol{D}(\boldsymbol{x}) + \boldsymbol{E}(\boldsymbol{x})\boldsymbol{u}$, we can compute the control law of the form

$$\boldsymbol{u} = \boldsymbol{E}^{-1}(\boldsymbol{x})(\boldsymbol{v} - \boldsymbol{D}(\boldsymbol{x}))$$

B. Linear Control for the Linearized System

Using the feedback linearization technique, the system (9) can be transformed into a system which, in suitable coordinates, is input-output linearized and controllable. The change of coordinates $\xi = \Phi(\boldsymbol{x})$ is given by

$$\begin{aligned} \xi_1 &= h_1(\boldsymbol{x}) = q_1 & \xi_4 &= L_f h_1(\boldsymbol{x}) = \dot{q}_1 \\ \xi_2 &= h_2(\boldsymbol{x}) = q_2 & \xi_5 &= L_f h_2(\boldsymbol{x}) = \dot{q}_2 \\ \xi_3 &= h_3(\boldsymbol{x}) = q_3 & \xi_6 &= L_f h_3(\boldsymbol{x}) = \dot{q}_3 \end{aligned}$$

In the new coordinates, the system appears as

$$\begin{aligned} \dot{\boldsymbol{\xi}} &= \boldsymbol{A}\boldsymbol{\xi} + \boldsymbol{B}\boldsymbol{v} \\ \boldsymbol{y} &= \boldsymbol{C}\boldsymbol{\xi} \end{aligned} \qquad (12)$$

in which, $\boldsymbol{\xi} = [\xi_1\ \xi_2\ \xi_3\ \xi_4\ \xi_5\ \xi_6]^T$, and

$$\boldsymbol{A} = \begin{bmatrix} \mathbf{0}_{3\times 3} & \mathbf{I}_{3\times 3} \\ \mathbf{0}_{3\times 3} & \mathbf{0}_{3\times 3} \end{bmatrix}$$

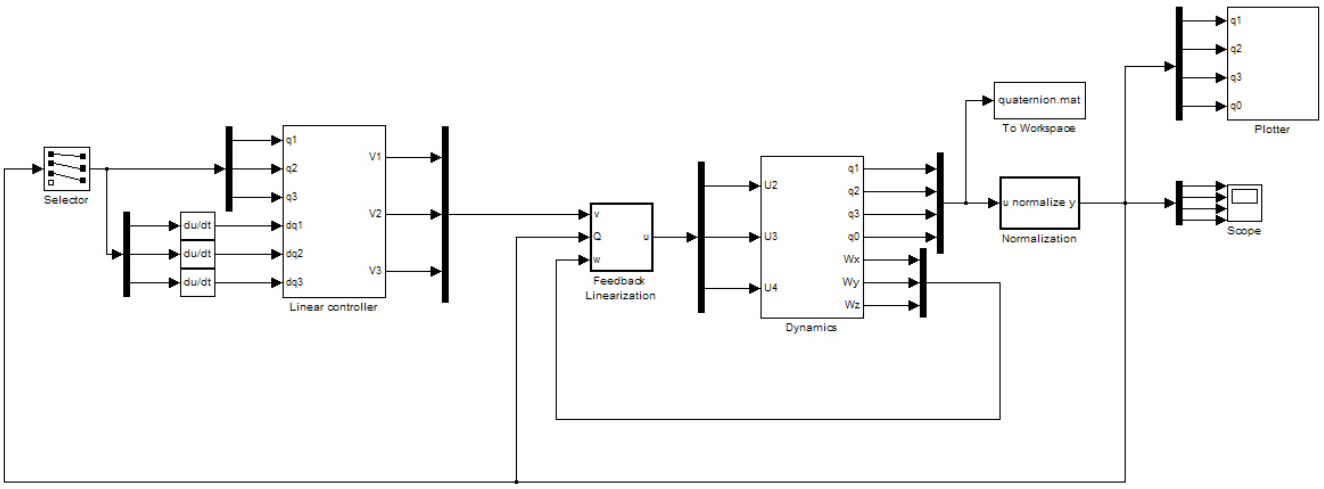

FIGURE 5. Block diagram of the control system built in Simulink

$$\boldsymbol{B} = \begin{bmatrix} \mathbf{0}_{3\times 3} \\ \mathbf{I}_{3\times 3} \end{bmatrix}$$

$$\boldsymbol{C} = \begin{bmatrix} \mathbf{I}_{3\times 3} & \mathbf{0}_{3\times 3} \end{bmatrix}$$

For the linear system (12), one can design a controller using a linear control law, which assigns the poles of the closed loop linear system to desired positions. The block diagram of the overall control system used here is shown in Fig. 5.

In the next section, simulations are carried out to verify the feasibility of the controllers proposed above.

C. Zero Dynamics Analysis

Note that the state variable q_0 is not connected to the output $\boldsymbol{y}$. In other words, the linearizing feedback control has made q_0 unobservable from $\boldsymbol{y}$. We must make sure that the variable q_0 is well behaved; that is, stable or bounded in some sense. This internal stability issue is addressed in the following by using the concept of zero dynamics [20].

The selection of the zero dynamics variable η has to satisfy two requirements: $z = \mathrm{T}(\boldsymbol{x}) = [\eta;\ \boldsymbol{\xi}]$ is a diffeomorphism and $\frac{\partial \eta}{\partial x}\mathrm{g}(\boldsymbol{x}) = 0$ [20]. Choose $\eta = q_0$, then

$$\frac{\partial \eta}{\partial \boldsymbol{x}} g(\boldsymbol{x}) = \begin{bmatrix} 1 & \mathbf{0}_{1\times 6} \end{bmatrix} \begin{bmatrix} & \mathbf{0}_{4\times 3} & \\ b_1 & 0 & 0 \\ 0 & b_2 & 0 \\ 0 & 0 & b_3 \end{bmatrix} = 0$$

In order to make sure that $z = \mathrm{T}(\boldsymbol{x}) = [\eta;\ \boldsymbol{\xi}]$ is a diffeomorphism, we can calculate the Jacobian matrix of z and its determinant as follows:

$$J(z) = \frac{\partial z}{\partial \boldsymbol{x}} = \begin{bmatrix} \mathbf{I}_{4\times 4} & \mathbf{0}_{4\times 3} \\ \boldsymbol{\Lambda}(\boldsymbol{\omega}) & Sk(\boldsymbol{Q}) \end{bmatrix}$$

where

$$\boldsymbol{\Lambda}(\boldsymbol{\omega}) = \begin{bmatrix} \frac{1}{2}\omega_x & 0 & \frac{1}{2}\omega_z & -\frac{1}{2}\omega_y \\ \frac{1}{2}\omega_y & -\frac{1}{2}\omega_z & 0 & \frac{1}{2}\omega_x \\ \frac{1}{2}\omega_z & \frac{1}{2}\omega_y & -\frac{1}{2}\omega_x & 0 \end{bmatrix}$$

$$Sk(\boldsymbol{Q}) = \begin{bmatrix} \frac{1}{2}q_0 & -\frac{1}{2}q_3 & \frac{1}{2}q_2 \\ \frac{1}{2}q_3 & \frac{1}{2}q_0 & -\frac{1}{2}q_1 \\ -\frac{1}{2}q_2 & \frac{1}{2}q_1 & \frac{1}{2}q_0 \end{bmatrix}$$

$$det(J(\boldsymbol{x})) = \tfrac{1}{8}q_0^3 + \tfrac{1}{8}q_0 q_1^2 + \tfrac{1}{8}q_0 q_2^2 + \tfrac{1}{8}q_0 q_3^2 = \tfrac{1}{8}q_0$$

When $q_0 \neq 0$, the Jacobian matrix is nonsingular and the zero dynamics satisfies the two requirements, so the system will be stable. In terms of the requirement for the matrix $\boldsymbol{E}(\boldsymbol{x})$ and the two requirements for the zero dynamics, we can conclude that the feedback linearization controller can work under the condition of $q_0 \neq 0$ ($q_0 = 0$ means that when expressed in the quaternion form, the rotation around an arbitrary 3D axis which is represented by the vector component of the quaternion is 180°; $q_0 = 1$ means that the Euler angles are stabilized to be 0).

TABLE 1. Omnicopter Attitude Stabilization Results

Roll ϕ_0	Pitch θ_0	Yaw ϕ_0	Roll ϕ_d	Pitch θ_d	Yaw ϕ_d	Convergence time (seconds)
70°	80°	90°	0°	0°	0°	1.8
30°	45°	60°	0°	0°	0°	1.5
30°	20°	10°	0°	0°	0°	1.6

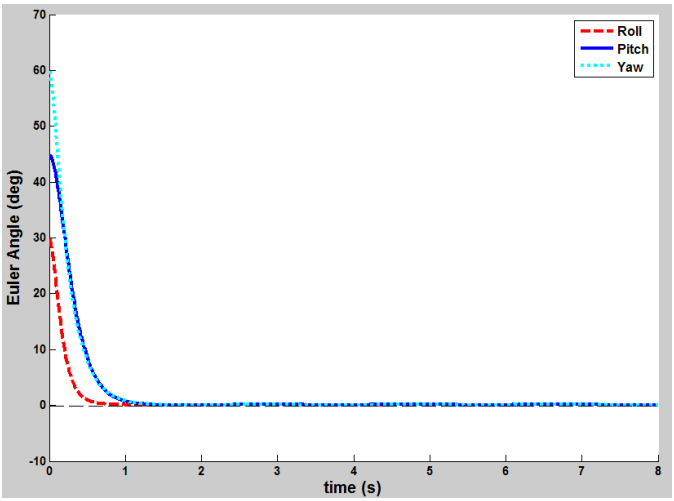

FIGURE 6. Attitude stabilization in the presence of signal noise and periodic disturbances with an amplitude of 0.08 *Nm*

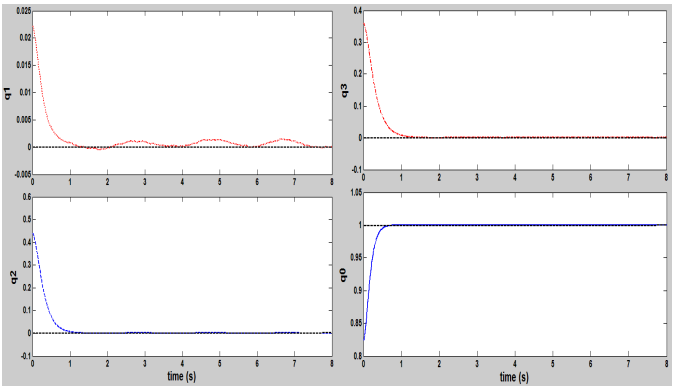

FIGURE 7. Quaternion components q_1 - q_3 converge to 0 and q_0 converges to 1 in the presence of noise and periodic disturbances with an amplitude of 0.08 *Nm*

V. SIMULATIONS AND ANALYSIS

Based on the control laws discussed, various simulations with different initial conditions were performed (see Table 1 for some examples). We found that with different initial conditions, the Euler angles can always be stabilized in a short convergence time, which proves the effectiveness of the proposed controller. Two of the results are presented in detail here to illustrate the performance of the proposed controller. Assume that the initial attitude is $[\phi_0\ \theta_0\ \psi_0]^T = [30^\circ\ 45^\circ\ 60^\circ]^T$, and the controller has to stabilize the attitude to the origin $[0\ 0\ 0]^T$. According to the transformation relation between the Euler angles and the quaternion [19], the equilibrium attitude, $[\phi_d\ \theta_d\ \psi_d]^T = [0\ 0\ 0]^T$, corresponds to $[q_0\ q_1\ q_2\ q_3]^T = [1\ 0\ 0\ 0]^T$.

To test the performance of the controller, in the first simulation, white noise with zero mean and 0.01 variance has been added to the angular velocity signals. The following periodic disturbances are also added to the attitude subsystem (7):

$$\boldsymbol{d} = \begin{bmatrix} \mu\sin(\pi t) + \mu\sin(\pi t/10) \\ \mu\sin(\pi t) + \mu\sin(\pi t/10) \\ \mu\sin(\pi t) + \mu\sin(\pi t/10) \end{bmatrix} Nm$$

where μ is chosen to be 0.08 *Nm*, 0.5 *Nm* and 3 *Nm* in different simulations. The results of these simulations are shown in Fig. 6-9. We can find that when the amplitude achieves 3 *Nm*, obvious periodic oscillation will happen. The controller will not be able

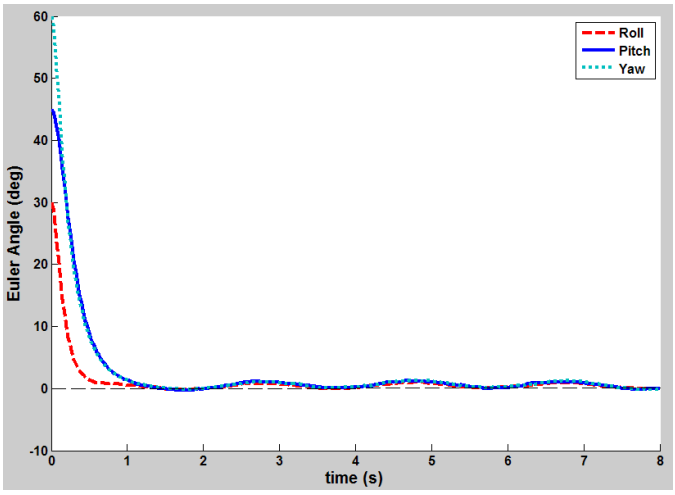

FIGURE 8. Attitude stabilization in the presence of signal noise and periodic disturbances with an amplitude of 0.5 *Nm*

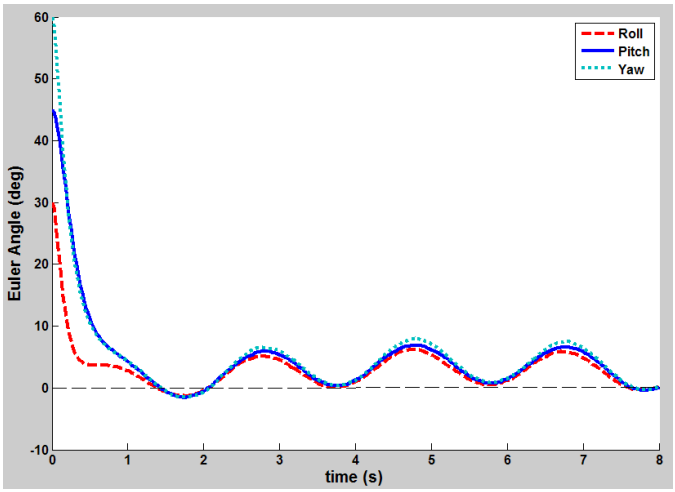

FIGURE 9. Attitude stabilization in the presence of signal noise and periodic disturbances with an amplitude of 3 *Nm*

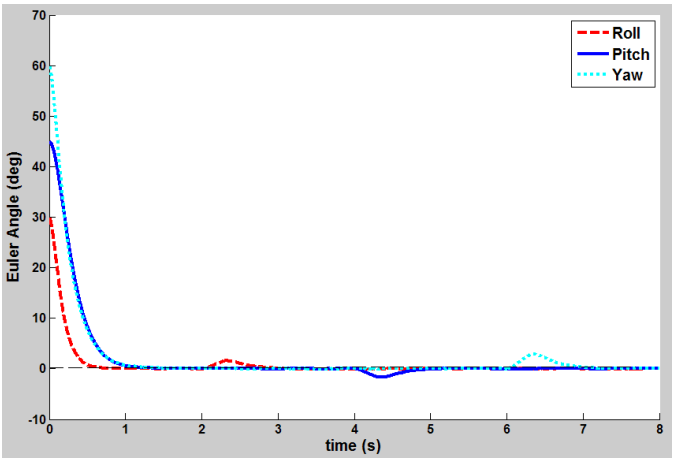

FIGURE 10. Attitude stabilization in the presence of signal noise and abrupt aerodynamic moment disturbances

to well stabilize the Omnicopter at that time.

In the second simulation, external disturbances on the aerodynamic moments were considered. When t $\in$ [2, 2.3)s, the disturbance A_p = 2 Nm was introduced, when t $\in$ [4, 4.3)s, the disturbance A_q = -2 Nm was introduced and when t $\in$ [6, 6.3)s, the last disturbance with an amplitude of A_r = 3 Nm was applied. These simulation results are pictured in Fig. 10. Thus, Fig. 6-10 show that the attitude can still be stabilized in the presence of sensor noise and periodic/abrupt moment disturbances.

VI. CONCLUSION

In this paper, the new Omnicopter MAV design has been presented. It is unique in its ability to withstand external disturbances and translate in the plane with a zero attitude, due to the lateral thrust vectors produced by its perimeter mounted variable angle ducted fans. A dynamic model of a coaxial MAV has been established using the Euler-Lagrange formalism. Then a feedback linearization controller has been developed for the special operating case with fixed vertical ducted fans. This controller renders the attitude subsystem linear and controllable from an input-output point of view. The simulation results prove that the attitude stabilization task for the Omnicopter is achieved in the presence of external disturbances.

The feedback linearization method used here depends on perfect knowledge of the system dynamics and uses that knowledge to cancel the nonlinearities of the system, but the system modeling is very difficult to be exact. Unmodelled dynamics, parameter uncertainties and unknown disturbances always exist, and therefore affect the cancelation of nonlinearities when using feedback linearization. In order to overcome the model inaccuracies, further investigation will be carried out on system identification and robust controllers. In addition, our future work will explore using the more advanced control method (M2), that is, control it by varying both angles and speeds of the ducted fans, for increased performance. A prototype will be constructed accordingly and the various control strategies will be experimentally verified on the platform.

REFERENCES

[1] Thorne, C., and Yim, M., 2011. "Towards the development of gyroscopically controlled micro air vehicles". *International Conference on Robotics and Automation, Shanghai, China,*, May.

[2] Escareno, J., Sanchez, A., Garcia, O., and Lozano, R., 2008. "Triple tilting rotor mini-uav: Modeling and embedded control of the attitude". *2008 American Control Conference*.

[3] Salazar-Cruz, S., Kendoul, F., Lozano, R., and Fantoni, I., 2006. "Real-time control of a small-scale helicopter having three rotors". *Proceedings of the 2006 IEEE/RSJ International Conference on Intelligent Robots and Systems*.

[4] Rongier, P., Lavarec, E., and Pierrot, F., 2005. "Kinematic and dynamic modeling and control of a 3-rotor aircraft". In Robotics and Automation, 2005. ICRA 2005. Proceedings of the 2005 IEEE International Conference on, pp. 2606 – 2611.

[5] Kim, J., Kang, M.-S., and Park, S., 2010. "Accurate modeling and robust hovering control for a quad-rotor vtol aircraft". *J Intell Robot Syst,* ***57:9-26***.

[6] Michael, N., Mellinger, D., Lindsey, Q., and Kumar, V., Sept. 2010. "The grasp multiple micro uav testbed". *IEEE Robotics and Automation Magazine*.

[7] Bouabdallah, S., Noth, A., and Siegwart, R., 2004. "Pid vs lq control techniques applied to an indoor micro quadrotor". *Proc. IEEE int. conf. on intelligent robots and systems,* ***3***, pp. 2451–2456.

[8] Raffo, G. V., Ortega, M. G., and Rubio, F. R., 2010. "An integral predictive/nonlinear h_∞ control structure for a quadrotor helicopter". *Automatica,* ***46:29-39***.

[9] Xu, R., and *Ü*mit *Ö*zgü*n*er, 2008. "Sliding mode control of a class of underactuated systems". *Automatica,* ***44:233-241***.

[10] Hoffmann, G., Rajnarayan, D., Wasl, S., and Tomlin, C., 2004. "The stanford testbed of autonomous rotorcraft for multi agent control (starmac". In In Proceedings of the 23rd Digital Avionics Systems Conference.

[11] Gress, G., 2002. "Using dual propellers as gyroscopes for tilt-prop hover control". *In Proc. AIAA Biennial Int. Powered Lift Conf. Exhibit, Williamsburg, VA*.

[12] Lim, K., and Moerder, D., 2007. "Cmg-augmented control of a hovering vtol platform". *AIAA Guidance, Navigation, and Control Conference and Exhibit, Hilton Head, SC*, August.

[13] Mistler, V., Benallegue, A., and M'Sirdi, N., 2001. "Exact linearization and noninteracting control of a 4 rotors helicopter via dynamic feedback". *IEEE International Workshop on Robot and Human Interactive Communication*.

[14] Benallegue, A., Mokhtari, A., and Fridman, L., May 2007. "High-order sliding-mode observer for a quadrotor uav". *International Journal of Robust and Nonlinear Control,* ***18:427-440***.

[15] Spong, M. W., Hutchinson, S., and Vidyasagar, M., 2006. *Robotic Modeling and Control*. John Wiley & Sons, Inc., 111 River Street, Hoboken, NJ 07030-5774.

[16] Ginsberg, J., 2008. *Engineering Dynamics*. Cambridge University Press, The Edinburgh Building, Cambridge CB2 8RU, UK.

[17] Zhenping, F., Wanchun, C., and Shuguang, Z., 2005. *Aerodynamics of Air Vehicles*. Beijing University of Aeronautics And Astronautics Press, Beijing, CN.

[18] Wu, S., Radice, G., Gao, Y., and Sun, Z., 2011. "Quaternion-based finite time control for spacecraft attitude tracking". *Acta Astronautica,* ***69:48-58***.

[19] Zhe, C., 1986. *Strapdown Inertial Navigation System Theory*. China Astronautic Publishing House, Beijing, CN.

[20] Khalil, H. K., 2002. *Nonlinear Systems*. Prentice Hall, Inc., Upper Saddle River, NJ 07458.